Journal of Biomedical Optics

BiomedicalOptics.SPIEDigitalLibrary.org

Au/NiFe/M(Au, MoS_2, graphene) trilayer magnetoplasmonics DNA-hybridized sensors with high record of sensitivity

Ehsan Faridi
Maryam Moradi
Narges Ansari
Amir Hossein Baradaran Ghasemi
Amir Afshar
Seyed Majid Mohseni

SPIE.

Ehsan Faridi, Maryam Moradi, Narges Ansari, Amir Hossein Baradaran Ghasemi, Amir Afshar, Seyed Majid Mohseni, "Au/NiFe/M(Au, MoS_2, graphene) trilayer magnetoplasmonics DNA-hybridized sensors with high record of sensitivity," *J. Biomed. Opt.* **22**(12), 127001 (2017), doi: 10.1117/1.JBO.22.12.127001.

Au/NiFe/M(Au, MoS_2, graphene) trilayer magnetoplasmonics DNA-hybridized sensors with high record of sensitivity

Ehsan Faridi,[a] Maryam Moradi,[b] Narges Ansari,[b,*] Amir Hossein Baradaran Ghasemi,[a] Amir Afshar,[a] and Seyed Majid Mohseni[a,*]
[a]Shahid Beheshti University, Faculty of Physics, G.C. Evin, Tehran, Iran
[b]Alzahra University, Department of Physics, Tehran, Iran

Abstract. The demonstration of biosensors based on the surface plasmon effect holds promise for future high-sensitive electrodeless biodetection. The combination of magnetic effects with surface plasmon waves brings additional freedom to improve sensitivity and signal selectivity. Stacking biosensors with two-dimensional (2-D) materials, e.g., graphene (Gr) and MoS_2, can influence plasmon waves and facilitate surface physiochemical properties as additional versatility aspects. We demonstrate magnetoplasmonic biosensors through the detuning of surface plasmon oscillation modes affected by magnetic effect via the presence of the NiFe (Py) layer and different light absorbers of Gr, MoS_2, and Au ultrathin layers in three stacks of Au/Py/M(MoS_2, Gr, Au) trilayers. We found minimum reflection, resonance angle shift, and transverse magneto-optical Kerr effect (TMOKE) responses of all sensors in the presence of the ss-DNA monolayer. Very few changes of $\sim 5 \times 10^{-7}$ in the ss-DNA's refractive index result in valuable TMOKE response. We found that the presence of three-layer Gr and two-layer MoS_2 on top of the Au/Py bilayer can dramatically increase the sensitivity by nine and four times, respectively, than the conventional Au/Co/Au trilayer. Our results show the highest reported DNA sensitivity based on the coupling of light with 2-D materials in magnetoplasmonic devices. © *2017 Society of Photo-Optical Instrumentation Engineers (SPIE)* [DOI: 10.1117/1.JBO.22.12.127001]

Keywords: magnetoplasmonic; magneto-optical-biosensor; DNA; MoS_2; graphene.

Paper 170478RR received Aug. 7, 2017; accepted for publication Nov. 16, 2017; published online Dec. 7, 2017.

1 Introduction

Surface plasmon resonance (SPR), the coherent oscillation of free electrons as a strongly localized charge density wave at a metal/dielectric interface, has had a strong scientific impact in nanoscale devices. This wave generates a large amplitude electric field, exponentially reducing from the main source at the interface. SPR is significantly influenced by the variation in the refractive index (RI)[1] of the surrounding environment closed by that metal/dielectric interface. It can thus be applied as a sensing mechanism.[2–4] SPR-based sensors are popular devices for sensing application due to the ease of measurement and fabrication technology,[5] and trustable prediction and verification ability by the electromagnetic wave propagation theory. Such SPR sensors and their underlying technology can potentially be applied in biology,[6–9] photovoltaic applications,[10] bioimaging,[11] controlling food safety,[12] and waveguides.[13,14]

For achieving high-resolution detectability and improving signal-to-noise amplitude, alternative techniques have been proposed to optimize the performance of SPR-based sensors. One promising technique was demonstrated on the controllability of SPR excitations via implementing a magnetic layer stacked within SPR elements to probe the reflected light polarization from devices, such as the magneto-optical Kerr effect (MOKE).[15,16] In addition to probing the reflection amplitude versus wavelength as well as angle, MOKE signal can be considered as a powerful mechanism, which is additionally sensitive to the magnetization of that magnetic layer and the external magnetic field. Thus, this type of sensing mechanism provides an additional detecting ability, resulting in better sensitivity compared with other conventional SPR sensors.[17]

Noble metallic thin films such as Au and Ag are typical materials frequently used for plasmonic application because of their high conductivity and chemical stability. However, these metals show a low MO response. In contrast, magnetic metals such as Co and Ni have a strong MO response, but they suffer from high optical losses.[18,19] Combining both magnetic and plasmonic functionalities, e.g., (Co or Ni)/(Au or Ag) bilayers as a hybrid magnetoplasmonic heterostructures, is a pioneering way to design SPR devices with great sensing performance. The enhancement of the MO signal by excitation of the SPR in magnetoplasmonic heterostructures was used to investigate biomolecules in a liquid,[20,21] weak field magnetic field sensor, memory,[22] and so on.

Recently, a great deal of interest has been made in optical devices to detect DNA and its hybridization development processes based on changes in its optical properties, toward recognition of genetic diseases,[23–25] and also to probe optical response of neurons toward cognitive investigations.[26] As a few examples, we can refer to the study of brain stimulation, where changes occur in the RI of stimulated neurons; optical properties of viruses against antibodies and the effects of drug release on cells, all can be probed via optical detection techniques.

*Address all correspondence to: Narges Ansari, E-mail: n.ansari@alzahra.ac.ir; Seyed Majid Mohseni, E-mail: m-mohseni@sbu.ac.ir

1083-3668/2017/$25.00 © 2017 SPIE

The optical sensor that we propose in this paper, which is sensitive to the RI of the environment, when it gets in contact with biological elements, needs to have suitable physiochemical properties, e.g., hydrophobicity, hydrophilicity, chemical stability, mechanical, electrical, and optical properties. Toward these requirements, two-dimensional (2-D) materials, e.g., graphene (Gr) and MoS_2, with a large specific surface area can be chemically functionalized properly to be satisfactorily implemented at the surface of optical sensors for accurate optical detection. It has been shown that Gr can interact with DNA through hydrogen bonding and π–π stacking force.[27] MoS_2 and the family of transition metal dichalcogenides can interact with DNA concentration through van der Waals force. Therefore, 2-D materials can be adjusted in a conducive way to interact with DNA.[28,29] In addition, such 2-D materials have exceptional optical properties[30,31] very suitable for application in hybridized SPR sensors.[32] For example, it was shown that the MoS_2 with resonance absorption peaks could significantly influence the MOKE detection signal in SPR sensors.[33]

To reiterate, the MO detection in magnetoplasmonics is highly sensitive to any changes in the RI of the environment. Moreover, impacts of adding 2-D materials of Gr or MoS_2 on such biosensors have not been investigated so far. Therefore, we introduce magnetoplasmonic biosensors including 2-D materials on top and in close contact with the DNA to be highly sensitive to any small changes in the RI of the DNA. In this paper, the MOKE response is calculated in SPR design including Au/NiFe/M(Au, MoS_2, Gr)/DNA to find optimized SPR and MOKE measurement results against any changes in the RI of DNA. We have shown that the NiFe, which is nominated as Permalloy (Py) is a quite sensitive layer against any small changes in applied magnetic field and thus very suitable for biological applications.[22,33] Here, based on the previously determined optimized thicknesses of Au(8 nm)/Py(13 nm) layers,[22,33] we vary the thicknesses of the Gr, MoS_2, and Au top layers, and study the details of angle-dependent reflectivity and MO response. We found that the presence of three-layer Gr and two-layer MoS_2 on top of the Au/Py bilayer can increase sensitivity by nine and four times, respectively. Our sensitivity achievements are much greater than any reported values using Au/Py/Au and Au/Co/Au stacks,[15,16] suggesting the important role of 2-D materials in the enhancement of biomolecule sensitivity in such sensors.

2 Theory

2.1 *Surface Plasmon Resonance Excitation and Transfer Matrix Method*

To excite the SPR by p-polarized light incident to interact between metal and dielectric medium, (i) the frequency of the incident light must be equal to the frequency of the SPR mode and (ii) the tangential component of the incident wave vector must be equal to the wave vector of the SPR. The most common approach to the excitation of the SPR is using a prism as a coupler between incident light and the SPR mode to study the attenuated total internal reflection method.[1]

In the presence of the magnetic field, the MO response of the magnetic layer is governed by the dielectric tensor. Up to first order in magnetization, the dielectric tensor in a transverse configuration can be read as

$$\overleftrightarrow{\varepsilon} = \begin{pmatrix} \varepsilon & 0 & 0 \\ 0 & \varepsilon & iaM \\ 0 & -iaM & \varepsilon \end{pmatrix}, \tag{1}$$

where M is the magnetization, a is the MO constant, and ε is the dielectric constant in the absence of magnetic field. The induced magnetization provides a nonreciprocal shift of k_{spp}, which causes a small change in the excitation angle and the intensity of reflected light. An expression for the plasmon excitation wave vector in the MO active layer when its thickness is adequately thin is

$$k_{\parallel}(\pm M) = k_{\parallel}^{0}\left[1 + \frac{2i}{\varepsilon^2 + 1}\left(\frac{\varepsilon}{\varepsilon + 1}\right)^{\frac{1}{2}}\left(\pm\frac{2\pi d}{\lambda}aM\right)\right], \tag{2}$$

where λ is the light wavelength in the vacuum and $k_{\parallel}^{0}$ is the wave vector of plasmon excitation in the absence of magnetic field. As can be deduced from Eq. (2), the induced magnetization causes the backward and forward modes to have different dispersion relations.

We employed the transfer matrix method (TMM) to numerically model the one-dimensional multilayer structures mentioned, and optimize their thicknesses to achieve the maximum MOKE sensitivity. We assumed that the light wave enters the initial (i) medium (i.e., the prism), passes through the multilayer structure, and exits from the final layer (f) (i.e., the water solution). By imposing the boundary conditions between tangential components of the electric and magnetic fields of the light wave, the relationship between the electric field amplitudes of the i and the f layer can be expressed as[34,35]

$$E_i = D_i^{-1}\prod_{n=1}^{N}[D_{(n)}P_{(n)}D_{(n)}^{-1}]D_f E_f \equiv \mathrm{ME}_f, \tag{3}$$

where E_i and E_f are the electric field amplitudes at the bottom surface of the i and the f media, $D_{(n)}$ is a boundary matrix including optical properties of the medium, and $P_{(n)}$ is the propagation matrix, which is dependent on the thickness of the layers

$$r_{pp} = \frac{M_{11}M_{43} - M_{13}M_{43}}{M_{11}M_{33} - M_{13}M_{31}}, \tag{4}$$

$$R_{pp} = |r_{pp}|^2, \tag{5}$$

where R_{pp} describes the intensity of reflected TM-polarized light.

The coupling between the incident light and the SPR can be changed when the magnetic field is applied. This results in a nonreciprocal effect on the SPR wave vector and the light reflection intensity when the magnetic field is reversed.[36] This effect is called the transverse MOKE (TMOKE), which is described by the following equation:

$$\frac{\Delta R_{pp}}{R_{pp}} = \frac{R_{pp}(+H) - R_{pp}(-H)}{R_{pp}(H = 0)}, \tag{6}$$

where H is the magnetic field and ΔR_{pp} and R_{pp} $(H = 0)$ are the pure optical and MO contributions of the TMOKE signal, respectively.

2.2 *Sensing Principle of TMOKE Biosensor*

When organic molecules are in contact with the surface of the SPR sensor, the interaction of the sensing layer with the biomolecules intends to change the optical responses of the sensing medium. Any changes within the RI of the medium can change the propagation vector of the SPR. Accordingly, the coupling condition between the incident light and the SPR will be different and the sensor output parameters will eventually vary.[2] The maximum sensitivity will be achieved when a tiny alteration in the medium RI causes a significant change in the output response of the sensor.

There are several detection mechanisms in SPR sensors. In sensors designed on the angle detection basis, the SPR is excited by monochromatic light at a short angle interval. The sensitivity is defined as the ratio of the resonance angle change to the RI change of the surrounding medium ($\eta_{\text{sensitivity}} = \delta\theta_{\text{spr}}/\delta n_d$). In other types of sensors based on wavelength modulation, the sensor is illuminated by polychromatic light at a fixed incident angle. The dip of the reflection spectrum corresponds to the SPR wavelength. Sensitivity is defined as the ratio of any shift in the resonance wavelength to the change in the RI of the sensing medium ($\eta_{\text{sensitivity}} = \delta\lambda_{\text{spr}}/\delta n_d$). In the third method, the intensity of reflection light serves as a sensor output. In this method, sensitivity is defined as the variation in the intensity of the output signal (S) at a fixed incident angle and fixed wavelength when n_d changes ($\eta_{\text{sensitivity}} = \delta S/\delta n_d$). The S parameter could be found based on R_{pp} detection (in conventional SPR measurement) or determined as the $\Delta R_{pp}/R_{pp}$ (in those based on TMOKE). For these methods, the shift in the position of SPR condition (θ_{spr}, λ_{spr}) and the changes in the detector signal intensity (R, $\Delta R_{pp}/R_{pp}$) are directly proportional to the change in the medium RI.

We first address the sensor's output performance, based on either TMOKE or the reflection response of the conventional Au/Py magnetoplasmonic biodetector. The bioelement we examine here is an immobilized single-stranded DNA (ss-DNA) with an RI of 1.462 (RI unit), which changes to double-stranded DNA (ds-DNA) with an RI of 1.530 (RI unit), based on any possible biological procedure actions.[37] It is to be noted that very little alteration within any biological procedures can change the RI of the ss-DNA. In our study, such changes occur at the top surface of the Py layer in the Au/Py bilayer magnetoplasmonic detector. We plot the TMOKE and reflection, Figs. 1(a) and 1(b), of such biosensors and compare their responses when a minute change affects RI of the ss-DNA. The detection mechanism could be based on intensity and angle changes in TMOKE signal and wavelength and reflection intensity all within the reflection light. These plots pedagogically picture the sensing mechanism on which we aim to improve detectivity later, based on adding different top layers in contact with biomolecules in continuation.

2.3 *TMOKE Sensor Structure*

In this paper, as already mentioned, we present a bilayer structure consisting of a noble and a ferromagnetic metal, Au/Py, which is located on the top of a prism in Kretschmann configuration. The structure was illuminated by a p-polarized and monochromic He–Ne laser. The schematics of proposed biosensors are shown in Fig. 2. The biosensing examination and sensitivity evaluation of such biosensors were carried out by adding a monolayer ss-DNA on top of the structures. The immobilized ss-DNA layer with a thickness of 3.3 nm, a density of 0.028 g/cm^2, and RI of 1.462 is located on the surface of the SPR biosensor and the whole structure is set in a water solution. In the proposed structures, based on our previous optimizations,[22,33] the thickness of the Au and Py layers is fixed at 8 and 13 nm, respectively. To compare the characteristics of conventional and 2-D material-based biosensors, we first obtain the reflection, MO, and sensitivity evaluation responses of the Au/Py bilayer structure. Next, we investigate the effect of 2-D materials Gr and MoS_2 and their replacement on the Au layer in three different structures, according to the designs in Fig. 2, and evaluate their responses for reflection, MO, and sensitivity.

We assume that the Gr and MoS_2 are isotropic media and the applied magnetic field does not affect their dielectric constants. The dielectric constants of Gr and MoS_2 at 633 nm wavelength are $\varepsilon_{\text{Gr}} = 7.6805 + 6.8922i$, $\varepsilon_{\text{MoS}_2} = 15.7987 + 5.6536i$, and their thicknesses are taken as $d_{\text{Gr}} = n_{\text{Gr}} \times 0.34\,(\text{nm})$, $d_{\text{MoS}_2} = n_{\text{MoS}_2} \times 0.65\,(\text{nm})$, respectively. Here we note that, n_G and n_{MoS_2} are numbers of the Gr and MoS_2 layers, respectively. A small magnetic field of about 20 (Oe) applied in the plane can saturate the Py layer. The real and imaginary components of the metal dielectric constant are calculated using the Lorentz–

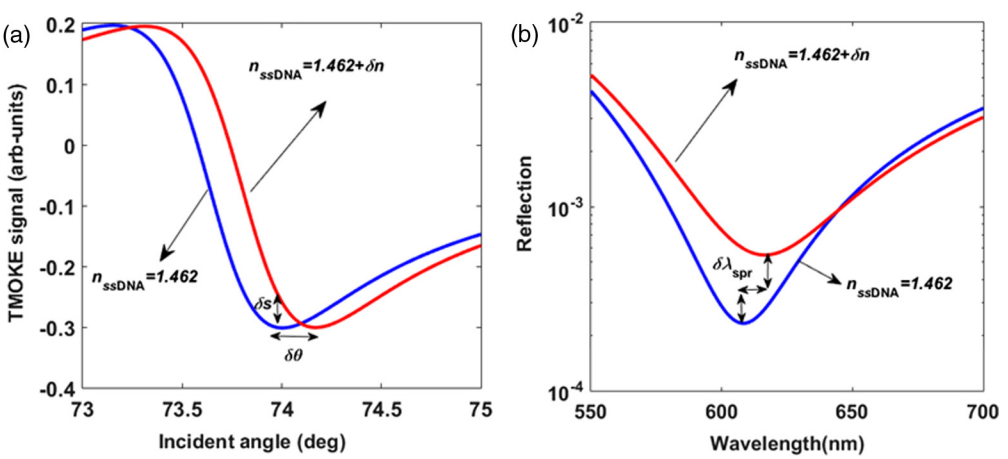

Fig. 1 (a) TMOKE response as a function of incident angle and (b) reflection of light as a function of wavelength in Au(8nm)/Py(13nm) bilayer having ss-DNA top layer. Any changes in RI of the ssDNA result in different responses of biosensor, plotted as blue and red colors. Here, we consider $\delta n = 0.068$.

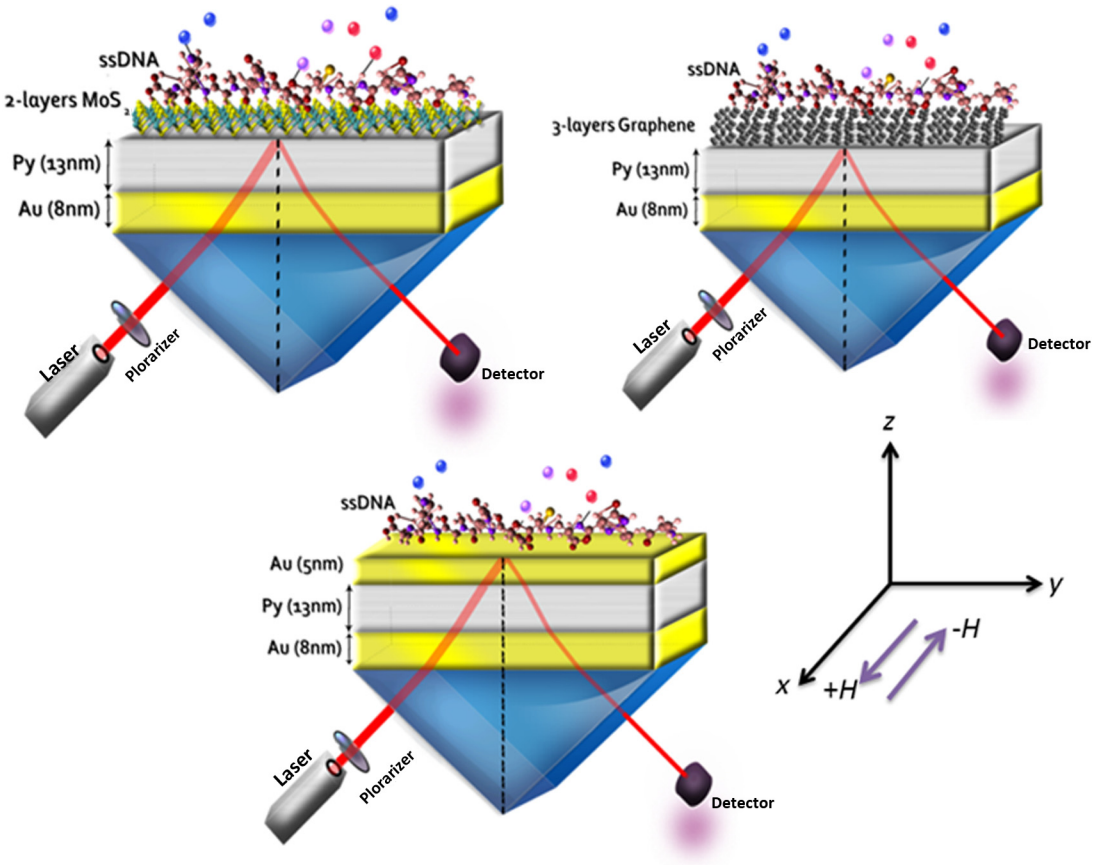

Fig. 2 Schematic illustration of presence of MoS_2, Gr, and Au top layer on Au/Py magnetoplasmonic biosensors in Kretschmann configuration. The bioelement, i.e., ss-DNA, is located on the SPR stacks as the top most layers. Laser light is incident from the bottom left, interacts with optical elements in the whole structure and gets reflected back to the detector positioned at the bottom right of the biosensor.

Drude model. In the case of Gr and MoS_2, we used the required parameters from Refs. 38 and 39. The wavelength dependencies of the layers' dielectric constant are plotted in Fig. 3. The complex dielectric constants of water, glass, Au, and Py at 632.8-nm wavelength are $\varepsilon_g = 2.2955$, $\varepsilon_{\text{water}} = 1.774$, $\varepsilon_{\text{Au}} = -10.2393 + 1.3694i$, and $\varepsilon_{\text{Py}} = -7.1481 + 17.7165i$, respectively. Furthermore, the MO constant of the magnetic Py layer is considered to be $\varepsilon_{xy} = -0.0960 + 0.2023i$.[40]

3 Biosensors' Responses

The reflectance and TMOKE responses as a function of the incident light angle are determined based on TMM for Au/Py/$MoS_2(\times n)$ layers, as shown in Fig. 4. The minima points observed in the reflection curves, Fig. 4(a), are attributed to the excitation of the SPR waves. The variation in the SPR excitation angle versus n is shown in Table 1. As we can see, the minima and the corresponding TMOKE signal strongly depend on the

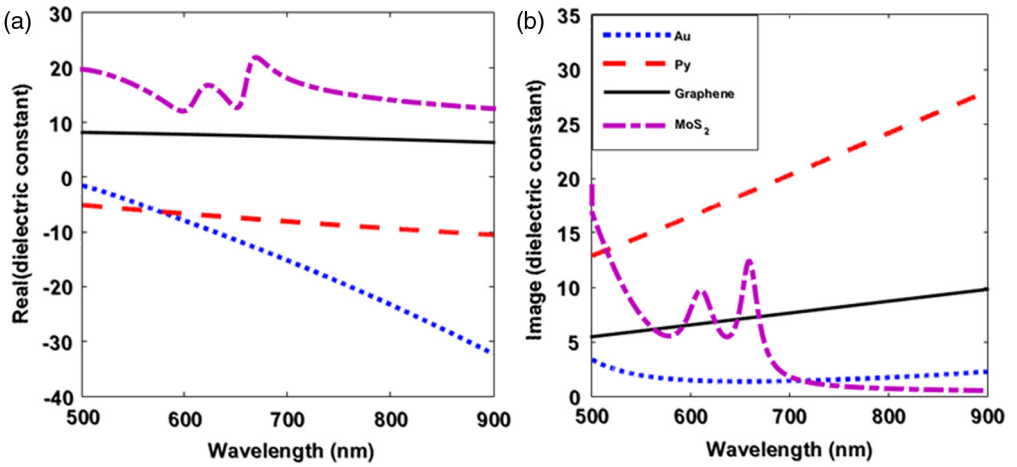

Fig. 3 (a) Real and (b) imaginary parts of dielectric constant of Au, Py, MoS_2, and Gr versus wavelength.

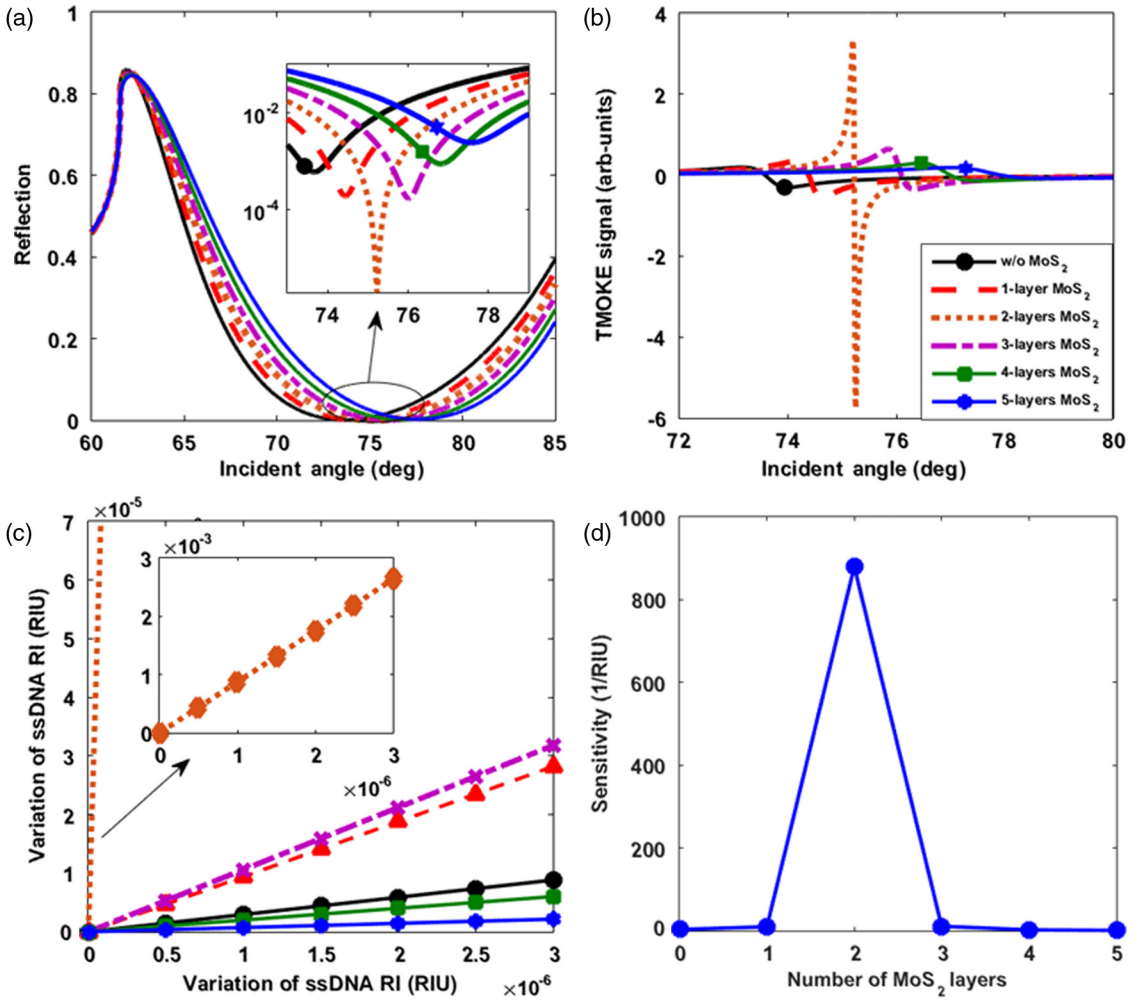

Fig. 4 (a) Reflection and (b) TMOKE signal versus incident angle. (c) TMOKE signal versus variation in the binding layer (ss-DNA) RI. (d) Sensitivity for Au/Py/MoS_2(×n)/ss-DNA versus *n*.

number of the MoS_2 layers. The maximum TMOKE signal is achieved in the structure that consists of two MoS_2 layers, and its value is 5.7. Owing to the ultranarrow behavior of the TMOKE signal versus angle at the SPR condition, the TMOKE signal can exhibit better sensitivity to RI variations than what reflection measures. We calculated a variation in the TMOKE signal when the RI of the binding layer increases due to the biochemical interaction and adsorption of the biomolecule. When the concentration occurs, the monolayer ss-DNA transforms to ds-DNA and its RI and density increase to 1.53 and 0.061 g/cm^2, respectively, as a result of densification and polarizability.

During the densification, we supposed that the changing of the binding layer of RI has a linear dependence on the enhancement of concentration. Moreover, we assumed that the RI increases from 1.462 to 1.4620030 by intervals of 5×10^{-7} (RIU). As can be observed in Fig. 4(c), when one layer of MoS_2 is deposited on the Au/Py bilayer, in addition to the enhancement of the TMOKE signal, the sensitivity of the proposed structure increases. The sensitivity information can be obtained by the slope of the TMOKE signal variations. The value of sensitivity is three times higher than in the structure without the MoS_2 layer. According to Fig. 4(b), in the presence of two MoS_2 layers, an extraordinary enhancement of both the TMOKE signal and sensitivity can be observed together with the approaching minimum reflection level as shown in Fig. 4(a). The enhancement of the TMOKE signal is due to the stronger excitation of the SPR waves,[33] and the sharp behavior of the TMOKE signal at the resonance condition is the reason for an increase in sensitivity. The numerical calculations predict that the sensitivity of the proposed sensor is $\eta = 880$ (RIU^{-1}). For structures consisting of more than two MoS_2 layers, the

Table 1 SPR angle for Au/Py/MoS_2(×n).

Au/Py/MoS_2(×n)	$n=0$	$n=1$	$n=2$	$n=3$	$n=4$	$n=5$
SPP angle (deg)	73.6	74.4	75.2	76	76.8	77.6

Table 2 SPR angle for Au/Py/Gr(×n).

Au/Py/Gr(×n)	$n=0$	$n=1$	$n=2$	$n=3$	$n=4$	$n=5$
SPP angle (deg)	73.6	73.9	74.2	74.5	74.7	75

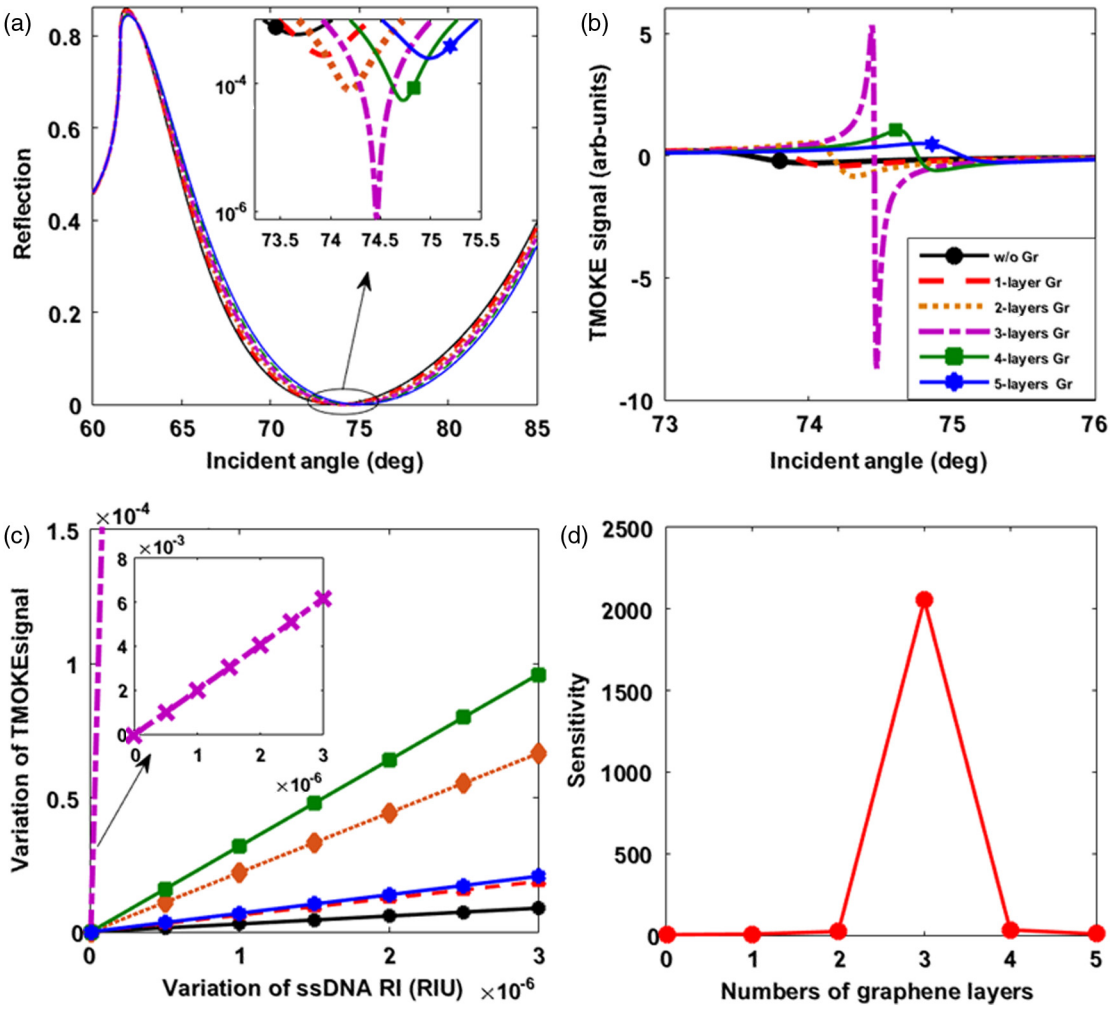

Fig. 5 (a) Reflection and (b) TMOKE signal versus incident angle. (c) TMOKE signal versus variation in the binding layer (ss-DNA) RI. (d) Sensitivity for Au/Py/Gr(×n)/ss-DNA versus n.

sensitivity has a notable reduction due to the increase in the optical dissipation of MoS_2.

Next, we calculate the effect of the Gr layers that are coated on the proposed Au/Py structure. The reflection, TMOKE signal, and sensitivity curves of Au/Py/Gr(×n)/ss-DNA are shown in Fig. 5 (different panels), where variation in the SPR excitation angle versus n is presented in Table 2. As compared with the SPR sensor with MoS_2 layers, the Gr absorbs biomolecules more strongly and stably due to the presence of π-stacking links. The lowest value of the resonance angle is smaller than the corresponding value with MoS_2, indicating better localization of the SPR waves. Dips of minima in the reflection shift to the large incident angle with an increase in the number of Gr layers. The shift of the resonance angle typically depends on both the numbers of the Gr layers as well as the value of the RI. The real part of Gr dielectric constant is smaller than that of MoS_2, and, hence, the shift in angle is smaller than that of MoS_2. In this case, the maximum value of sensitivity is obtained when three layers of Gr are coated on the Au/Py SPR structure, and its value is found to be $\eta = 2056$ (RIU^{-1}), which is 2.3 times greater than the highest value attained with the MoS_2 top layer design.

Table 3 SPR angle for Au/Py/Au[t(nm)].

Au/Py/Au[t(nm)]	$t=0$	$t=1$	$t=2$	$t=3$	$t=4$	$t=5$	$t=6$
SPP angle (deg)	73.6	73.7	73.8	73.9	74	74.05	74.1

We have additionally compared our biosensors designed with 2-D-material of Gr and MoS_2 with a conventional planar trilayer Au/Py/Au_{top}, and the results are shown in Fig. 6. We calculated the reflection of Au/Py/Au[t(nm)] for six different thickness values of the top Au layer. According to the results in Fig. 6(a) and Table 3, the minimum depth decreases with an increase in the thickness of Au film. Similarly, the TMOKE signal, Fig. 6(b), at SPR condition increases with an increase in the Au thickness. The optimized thickness for Au_{top} is 5 (nm). The maximum sensitivity determined in Fig. 6(d) for this configuration is $\eta = 287$ (RIU^{-1}), which is substantially lower than the configurations that have Gr and MoS_2 layers.

To compare our sensitivity calculations with those of other designs,[15,16] the highest sensitivity determined based on optimized parameters in our various configurations is shown in Fig. 7. As we can see, the value of sensitivity in structures with Gr and MoS_2 is much greater than those obtained in other biosensors with mainly Au/Co/Au stacks. For example, for structure including of three-layer Gr and two-layer MoS_2, the

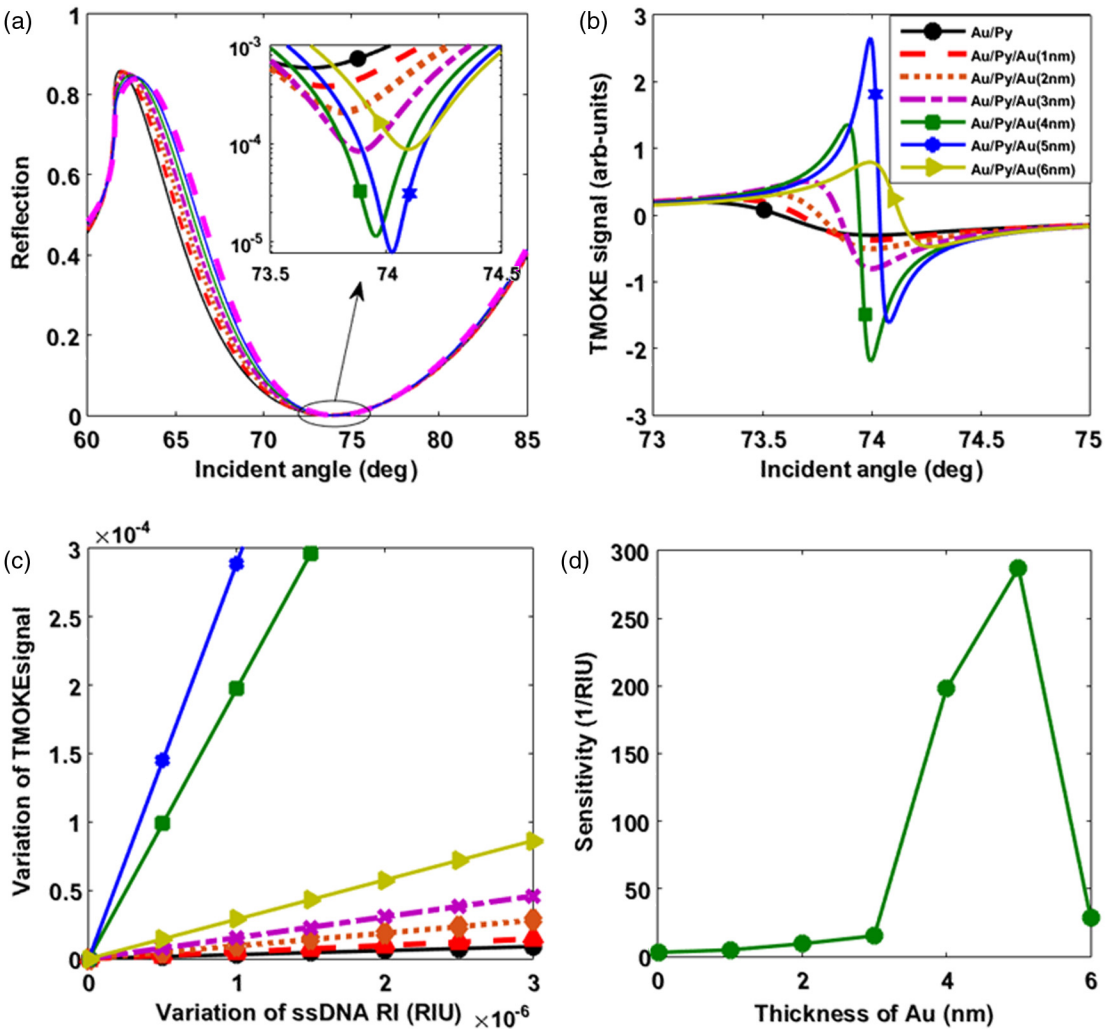

Fig. 6 (a) Reflection and (b) TMOKE signal versus incident angle. (c) TMOKE signal versus variation in the binding layer (ss-DNA) RI. (d) Sensitivity for Au/Py/Au[t(nm)]/ss-DNA versus Au_{top} thicknesses.

coupling between incident wave and surface plasmon is much stronger than that of other structures. This strong coupling leads to a large enhancement of the TMOKE signal. Furthermore, TMOKE signal gets sharper when the coupling becomes stronger. This sharp behavior causes TMOKE signal to become more sensitive to the change of the RI.

In addition to the sensitivity record values obtained here, we maintain that the Gr or MoS_2 top layers have already been found to be interesting materials because of their alternative physiochemical properties, which are suitable for biology.

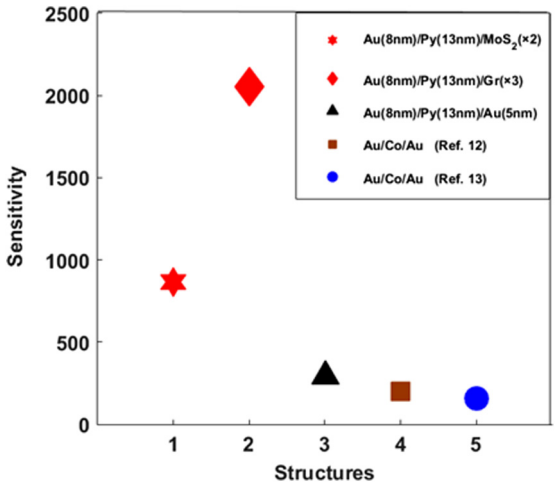

Fig. 7 A comparison between different designs of our magnetoplasmonic biosensors and those reported values in Refs. 15 and 16.

4 Conclusion

The development of biosensors with improved quality, biocompatibility, selectivity, and sensitivity requires state-of-the-art material with alternative physical and chemical properties. The application of well-known 2-D materials such as Gr and MoS_2 can guarantee such advantages. We demonstrate stacks of trilayers mainly made of Au/Py/M, where M (MoS_2 and Gr layers compared with the commonly used Au layer) is the layer in contact with biomolecules. We have shown reflection and TMOKE to be quite sensitive to small changes in the RI of the environment and biomolecules. The maximum sensitivity was found in stacks with top layers, which included two-layer MoS_2, three-layer Gr, and 5 nm Au to be $\eta = 880$, 2056, and 287 (RIU^{-1}), respectively. The degree of shift in dips of the reflection was found to be highly affected by the real component of the RI of each layer. Our determined values of sensitivity are the best recorded so far among those obtained in magnetoplasmonic

biosensor stacks. We believe our biosensor designs and their achievements are useful for future developments in their application in multitask optical-based biodetectors, which enable additional advantages and versatility, based on their alternative physiochemical properties.

Disclosures

The authors have no financial interests or conflicts of interest to disclose.

Acknowledgments

N.A. acknowledges support from Alzahra University research deputy. S.M.M. acknowledges support from Iran Science Elites Federation (ISEF), Iran's National Elites Foundation (INEF), and Iran's Cognitive Sciences and Technologies Council under Contract No. 2714.

References

1. H. Raether, *Surface Plasmons on Smooth and Rough Surfaces and on Gratings*, Springer, Berlin, Heidelberg (1988).
2. J. Homola and M. Piliarik, "Surface plasmon resonance (SPR) sensors," *Springer Ser. Chem. Sens. Biosens.* **4**, 45–67 (2006).
3. S. Zeng et al., "Graphene-MoS_2 hybrid nanostructures enhanced surface plasmon resonance biosensors," *Sens. Actuators B Chem.* **207**, 801–810 (2015).
4. A. K. Sharma and G. J. Mohr, "Plasmonic optical sensor for determination of refractive index of human skin tissues," *Sens. Actuators B Chem.* **226**, 312–317 (2016).
5. J. Homola, S. S. Yee, and G. Gauglitz, "Surface plasmon resonance sensors: review," *Sens. Actuators B Chem.* **54**(1), 3–15 (1999).
6. K. Kim et al., "Localized surface plasmon resonance detection of layered biointeractions on metallic subwavelength nanogratings," *Nanotechnology* **20**(31), 315501 (2009).
7. P. Otipka, J. Vlček, and M. Lesňák, "Designing of MO-SPR bio-chip with photonic crystal," *Proc. SPIE* **10142**, 101421V (2016).
8. R. Iovine, L. La Spada, and L. Vegni, "Nanoplasmonic sensor for chemical measurements," *Proc. SPIE* **8774**, 877411 (2013).
9. A. Tomitaka et al., "Development of magneto-plasmonic nanoparticles for multimodal image-guided therapy to the brain," *Nanoscale* **9**(2), 764–773 (2017).
10. S. Mubeen et al., "On the plasmonic photovoltaic," *ACS Nano* **8**(6), 6066–6073 (2014).
11. M. Kikawada et al., "Enhanced multicolor fluorescence in bioimaging using deep-ultraviolet surface plasmon resonance," *Appl. Phys. Lett.* **104**(22), 223703 (2014).
12. K. Narsaiah et al., "Optical biosensors for food quality and safety assurance—a review," *J. Food Sci. Technol.* **49**(4), 383–406 (2012).
13. A. K. Sheridan et al., "Waveguide surface plasmon resonance sensing: electrochemical desorption of alkane thiol monolayers," *Sens. Actuators B Chem.* **117**(1), 253–260 (2006).
14. T. Viitala et al., "Fluid dynamics modeling for synchronizing surface plasmon resonance and quartz crystal microbalance as tools for biomolecular and targeted drug delivery studies," *J. Colloid Interface Sci.* **378**(1), 251–259 (2012).
15. C. Rizal, "Bio-magnetoplasmonics, emerging biomedical technologies and beyond," *J. Nanomed. Res.* **3**(3), 00059 (2016).
16. M. G. Manera et al., "Enhanced antibody recognition with a magneto-optic surface plasmon resonance (MO-SPR) sensor," *Biosens. Bioelectron.* **58**, 114–120 (2014).
17. M. Moradi, Z. Ayareh, and M. G. Mahmoodi, "Enhancement of magneto-optical Kerr response by LSPR in magneto plasmonic nanostructures for biological sensors," *J. Magn. Magn. Mater.* **444**, 410–415 (2017).
18. V. I. Belotelov, L. L. Doskolovich, and A. K. Zvezdin, "Extraordinary magneto-optical effects and transmission through metal-dielectric plasmonic systems," *Phys. Rev. Lett.* **98**(7), 077401 (2007).
19. B. Sepúlveda et al., "Plasmon-induced magneto-optical activity in nanosized gold disks," *Phys. Rev. Lett.* **104**(14), 147401 (2010).
20. B. Sepúlveda et al., "Highly sensitive detection of biomolecules with the magneto-optic surface-plasmon-resonance sensor," *Opt. Lett.* **31**(8), 1085–1087 (2006).
21. S. David et al., "Magneto-plasmonic biosensor with enhanced analytical response and stability," *Biosens. Bioelectron.* **63**, 525–532 (2015).
22. M. Moradi et al., "Au/NiFe magnetoplasmonics: large enhancement of magneto-optical Kerr effect for magnetic field sensors and memories," *Electron. Mater. Lett.* **11**(3), 440–446 (2015).
23. K. V. Sreekanth et al., "Sensitivity enhanced biosensor using graphene-based one-dimensional photonic crystal," *Sens. Actuators B Chem.* **182**, 424–428 (2013).
24. J. Hottin et al., "Plasmonic DNA: towards genetic diagnosis chips," *Plasmonics* **2**(4), 201–215 (2007).
25. S. A. Kim et al., "Surface-enhanced localized surface plasmon resonance biosensing of avian influenza DNA hybridization using subwavelength metallic nanoarrays," *Nanotechnology* **22**(28), 289501 (2011).
26. F. Sohrabi and S. M. Hamidi, "Neuroplasmonics: from Kretschmann configuration to plasmonic crystals," *Eur. Phys. J. Plus* **131**(7), 221 (2016).
27. P. T. K. Loan et al., "Graphene/MoS_2 heterostructures for ultrasensitive detection of DNA hybridisation," *Adv. Mater.* **26**(28), 4838–4844 (2014).
28. C. Lu et al., "Comparison of graphene oxide and reduced graphene oxide for DNA adsorption and sensing," *Langmuir* **32**(41), 10776–10783 (2016).
29. B. L. Li et al., "Low-dimensional transition metal dichalcogenide nanostructures based sensors," *Adv. Funct. Mater.* **26**(39), 7034–7056 (2016).
30. N. Ansari and E. Mohebbi, "Increasing optical absorption in one-dimensional photonic crystals including MoS_2 monolayer for photovoltaics applications," *Opt. Mater.* **62**, 152–158 (2016).
31. N. Ansari and M. Moradi, "Optical absorption in air/monolayer MoS_2/S (S = SiO_2 or Si) trilayer stacks at oblique incidence," *Superlattices Microstruct.* **104**, 104–111 (2017).
32. E. Faridi and S. M. Mohseni, "Voltage-driven magneto-optical Kerr effect in a glass/Au/NiFe/dielectric/WS_2 magneto-plasmonic structure," *J. Opt. Soc. Am. B* **34**(12), 2436–2440 (2017).
33. A. H. B. Ghasemi et al., "Extraordinary magneto-optical Kerr effect via MoS_2 monolayer in Au/Py/MoS_2 plasmonic cavity," *RSC Adv.* **6**(108), 106591–106599 (2016).
34. S. Visnovsky et al., "Magnetooptic ellipsometry in multilayers at arbitrary magnetization," *Opt. Express* **9**(3), 121–135 (2001).
35. J. Zak et al., "Fundamental magneto-optics," *J. Appl. Phys.* **68**(8), 4203–4207 (1990).
36. V. Zayets et al., "Enhancement of the transverse non-reciprocal magneto-optical effect," *J. Appl. Phys.* **111**(2), 023103 (2012).
37. S. Elhadj, G. Singh, and R. F. Saraf, "Optical properties of an immobilized DNA monolayer from 255 to 700 nm," *Langmuir* **20**(13), 5539–5543 (2004).
38. B. Mukherjee et al., "Complex electrical permittivity of the monolayer molybdenum disulfide (MoS_2) in near UV and visible," *Opt. Mater. Express* **5**(2), 447–455 (2015).
39. M. Bruna and S. Borini, "Optical constants of graphene layers in the visible range," *Appl. Phys. Lett.* **94**(3), 031901 (2009).
40. E. D. Palik, *Handbook of Optical Constants of Solids*, p. 989, Academic Press, San Diego (1997).

Biographies for the authors are not available.